

# The role of interfacial friction on the peeling of thin viscoelastic tapes

M. Ceglie,<sup>1</sup> N. Menga,<sup>1,2,\*</sup> and G. Carbone<sup>1,2</sup>

<sup>1</sup>*Department of Mechanics, Mathematics and Management,  
Politecnico of Bari, V.le Japigia, 182, 70126, Bari, Italy*

<sup>2</sup>*Imperial College London, Department of Mechanical Engineering,  
Exhibition Road, London SW7 2AZ*

## Abstract

We study the peeling process of a thin viscoelastic tape from a rigid substrate. Two different boundary conditions are considered at the interface between the tape and the substrate: stuck adhesion, and relative sliding in the presence of frictional shear stress. In the case of perfectly sticking interface, we found that the viscoelastic peeling behavior resembles the classical Kendall behavior of elastic tapes, with elastic modulus given by the tape high-frequency viscoelastic modulus. Including the effect of frictional sliding, which occurs at the interface contiguous to the peeling front, makes the peeling behavior strongly dependent on the peeling velocity. We also predict a significant toughening of the peeling process, that occurs when the peeling angle is reduced to sufficiently small values. This phenomenon is in agreement with recent experimental results related to the low-angle peeling of elastic tapes under frictional sliding at the interface, which have been regarded as a possible mechanism exploited by biological systems (e.g. geckos, spiders) in controlling attachment force and locomotion.

Keywords: peeling, viscoelasticity, interfacial friction, adhesion

---

\*Electronic address: nicola.menga@poliba.it

## I. INTRODUCTION

The ability to control the mechanical behavior of real interfaces is one of the most challenging topic in modern industrial engineering, as witnessed by the restless effort made in the last decades in elastic [1–8], viscoelastic [9–16] and adhesive [17–24] contact mechanics studies. In this respect, the functionality of several real-life devices such as, for instance, pressure sensitive adhesives, modern touch screens, biomedical wound dressing and Band-Aids, is tightly connected to the possibility of tailoring the strength of interfacial adhesion between these systems and the mating surfaces. Therefore, the attachment/detachment performance of such interfaces are of primary concern. Among the possible detachment mechanisms, peeling is usually regarded as one of the most important [25] as it offers the chance to independently variate both the peeling load  $P$  and the peeling angle  $\theta$ . Due to its reliability, also the adhesive performance of industrial interfaces is often performed via opportunely designed peeling tests [26]. For these reasons, a deep understanding of the physics behind peeling processes is of primary importance in modern engineering.

The basic understanding of the peeling behavior of thin elastic tapes is nowadays well established. Indeed, Kaelble's [27–29] and Kendall's [30] studies set the theoretical framework to investigate the peeling evolution by relying on energy balance of the system. Their pioneeristic results were valid under specific hypothesis, such as the linear elasticity of the tape, perfect interfacial backing between the tape and the substrate, negligible tape bending stiffness. However, in the last decades, most of the original assumptions have been relaxed in successive studies. It is the case, for instance, of the effect of bending stiffness in thick tapes, which has been investigated in Refs [31, 32] in the presence of viscous losses occurring in the adhesive layer and in the tape. In Refs [33, 34] the effect of the substrate viscoelasticity on the peeling behavior has been studied to show that the steady detachment speed can be tuned under specific conditions and ultratough peeling may occurs at low peeling angles. The effect of the tape viscoelasticity has been investigated in Ref. [35–38] where it has been shown that the peeling force can be related to the peeling velocity  $V$  by an empirical relationship in the form  $P \approx kV^n$ , which holds true on a limited range of peeling velocities [25].

Beside viscoelasticity also the tape-substrate interfacial interactions play a fundamental role in determining the evolution of the peeling process, as already observed by Kendall [39, 40], who showed that interfacial sliding between the tape and the substrate may trigger cyclic detachment and re-attachment of the tape. Nonetheless, such a relative slippage represents an additional source of energy dissipation due to frictional shear stress occurring at the interface [41, 42], which has been investigated in details in the case of elastic tapes peeled away from rigid substrates under frictionless [44] and frictional [43] sliding. Theoretical and experimental investigations have concluded that, as expected, the presence of frictional sliding at the interface leads to significantly higher peeling force which may theoretically diverge at vanishing peeling angle. It has been suggested that the enhancement of peeling force caused by energy dissipated in frictional sliding plays a key role in biological applications. Indeed, several studies have identified this mechanism as one of the sources of the superior adhesive performance of the geckos [45–47], insects [48, 57] and frogs [49], beside the well investigated effect of the hierarchical nature of the attachment pads of these animals [50–52]. Moreover V-shaped peeling configuration observed in such biological systems [53–56] plays also a role in facilitating the ability of climbing animals to easily switch between firm attachment and effortless detachment. The resulting peeling force arises due

to the combination of three main physical mechanisms [59]: (i) tape pre-strain due to partial sliding occurring during detachment [60, 61]; (ii) the friction losses associated with the slip at the interface [58]; (iii) the viscous dissipation in the bulk of the material [62]. Interestingly, the last contribution is usually ascribed to the viscous shear of the interfacial thin fluid film formed by the pad secretion [63, 64]; however, a comprehensive model on the effect of the pad tissue bulk viscoelasticity [65, 66] on the overall frictional peeling is lacking.

In this study, we present a theoretical model of the behavior of a thin viscoelastic tape peeled away from a rigid substrate. Specifically, we aim at investigating the combined effect of frictional interfacial sliding occurring during the detachment process and the energy dissipation associated with the viscoelastic behavior of the tape. In order to shed light on the interplay between these mechanisms of energy dissipation, we consider two different configurations: (i) first, we focus on the case of no frictional sliding between the adhered part of the tape and the substrate (fully stuck conditions), (ii) then, we introduce the frictional sliding. Our findings may be of help to estimate the effect of the bulk viscoelasticity of bio-inspired and natural systems (e.g. biological fibrils, industrial polymeric tapes, etc.) on their overall peeling behavior in the presence of interfacial frictional slippage.

## II. FORMULATION

In this section, we present the mathematical model for the viscoelastic peeling assuming two different conditions at the interface between the tape and the rigid substrate: (i) stuck adhesion, where tape normal and tangential displacements are inhibited; (ii) relative frictional sliding, i.e. tape normal displacements are inhibited but tangential sliding occurs in the presence of frictional shear stresses. In both cases, the problem formulation builds on energy balance. We focus on a linear viscoelastic material with a single relaxation time  $t_c$ . Further, we neglect any dynamic effect during the tape detaching process (*i.e.* we assume that the peeling front velocity is far lower than the speed of sound in the tape).

### Stuck interface

Consider a viscoelastic tape, of thickness  $d$  and transversal width  $b$ , baked onto a rigid substrate with no relative sliding at the interface. As shown in Fig. 1, the tape is peeled away at an angle  $\theta$  under a constant force  $P$ . We assume the peeling front moves on the left at a constant velocity  $V_0$  relative to the substrate. We observe the peeling process from an observer fixed to the peeling front. In such reference frame, the substrate moves on the right at speed  $V_0$  as shown in 1.

Under steady state conditions, the energy balance per unit time of the viscoelastic tape is given by

$$W_E + W_I + W_S = 0 \tag{1}$$

where  $W_E$  is the work per unit time of the external forces acting on the tape,  $W_I$  is work per unit time done by the stress acting into the tape material, and  $W_S$  is the work per unit time done by interfacial forces.

The term  $W_E$  in Eq. (1) can be calculated considering the external forces acting on the system, which are the remote load  $P$  acting on the detached tape tip, and the corresponding

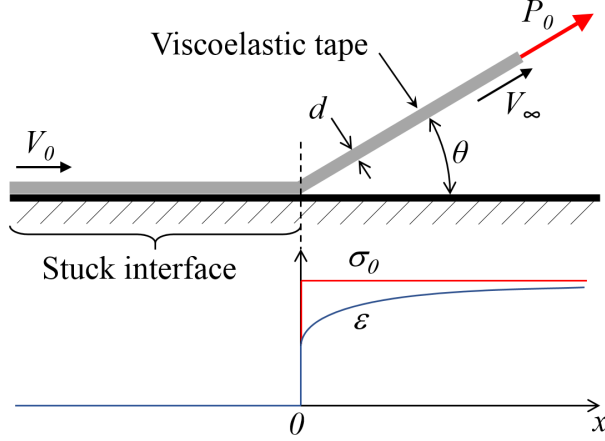


FIG. 1: The scheme of the peeling process of a thin viscoelastic layer from a rigid substrate in the presence of stuck adhesion at the interface, so that no relative sliding occurs. In the lower part, qualitative diagrams of the tape stress  $\sigma$  (red) and deformation  $\varepsilon$  (blue) are shown.

substrate reaction force  $-P \cos \theta$ . We have

$$W_E = PV_\infty - PV_0 \cos \theta = \sigma_0 V_0 b d \left( 1 + \frac{\sigma_0}{E_0} - \cos \theta \right) \quad (2)$$

where we defined  $\sigma_0 = P/bd$ . Moreover, the mass balance of the tape gives  $V_\infty = V_0(1 + \sigma_0/E_0)$ . Notably, in Eq. (2) we assumed that the tape tip (where the force  $P$  is applied) is located sufficiently far from the peeling front, so that complete viscoelastic relaxation occurs in the detached tape.

The surface term  $W_S$  in Eq. (1) represents the energy per unit time associated with the rupture of interfacial adhesive bond, with  $\Delta\gamma$  being the work of adhesion needed to detach a unit surface of the tape from the substrate. Although,  $\Delta\gamma$  may also depend on local irreversible nonlinear phenomena occurring at the peeling front (the so-called crack tip process zone), for the sake of simplicity, here we neglect such nonlinear effects, thus assuming a constant  $\Delta\gamma$  value. Therefore, we can write

$$W_S = -\Delta\gamma b V_0 \quad (3)$$

The term  $W_I$  in Eq. (1) takes into account both the elastic energy stored in the tape, and the bulk energy dissipation occurring due to viscoelastic creep in the detached strip. Since we focus on thin tapes, we can neglect the bending contribution to  $W_I$  (see also Refs [54, 55]). Hence we write

$$W_I = -V_0 b d \int_{-\infty}^{+\infty} \sigma(x) \varepsilon'(x) dx \quad (4)$$

where  $\varepsilon'(x)$  is the spatial derivative of the strain  $\varepsilon(x)$ . Note that, in Eq. (4), we used  $\dot{\varepsilon}(x) = V_0 \varepsilon'(x)$ , with  $\dot{\varepsilon}(x)$  being the time derivative of  $\varepsilon(x)$ .

Since in this section we assume no interfacial sliding between the adhering tape and the rigid substrate, the stress distribution in the viscoelastic tape is given by  $\sigma(x) = \sigma_0 H(x)$ ,

with  $H(x)$  being the Heaviside step function (see the diagram in Fig. 1). Moving from the linear viscoelastic constitutive equation [67], in the framework of steady state conditions, the deformation field can be calculated as

$$\varepsilon(x) = \int_{-\infty}^x J(x-s)\sigma'(s) ds \quad (5)$$

where  $J(x)$  is the spatial transformation of the viscoelastic creep function given by

$$J(x) = H(x) \left[ \frac{1}{E_0} - \frac{1}{E_1} \exp\left(-\frac{x}{\lambda}\right) \right] \quad (6)$$

where  $\lambda = V_0 t_c$  is the relaxation length, and  $E_1^{-1} = E_0^{-1} - E_\infty^{-1}$  with  $E_0$  and  $E_\infty$  being the low and very high frequency viscoelastic moduli, respectively.

For the case at hand, Eq. (5) gives  $\varepsilon(x) = \sigma_0 J(x)$ , which substituting into Eq. (4), after some algebra, gives

$$W_I = -V_0 b d \sigma_0^2 \left( \frac{1}{E_0} - \frac{1}{2E_\infty} \right) = -\frac{V_0 b d \sigma_0^2}{2} \left( \frac{1}{E_0} + \frac{1}{E_1} \right) \quad (7)$$

where we have used that  $\int_{-\infty}^{+\infty} \delta(x)H(x) dx = 1/2$ , which gives  $\varepsilon(0) = \frac{1}{2} [\varepsilon(0^-) + \varepsilon(0^+)] = \frac{1}{2}\varepsilon(0^+)$ . Note that the viscoelastic dissipated energy per unit time is

$$D_s = \frac{V_0 b d \sigma_0^2}{2E_1} \quad (8)$$

Finally, substituting Eqs. (2,3,7) into Eq. (1) we have

$$\frac{\sigma_0^2}{2E_\infty} + \sigma_0(1 - \cos \theta) = \frac{\Delta\gamma}{d} \quad (9)$$

which represents the peeling equilibrium condition. Interestingly regardless of the peeling velocity  $V_0$ , Eq.(9) is identical to the Kendall equation with the low frequency viscoelastic modulus  $E_0$  replaced by the high frequency viscoelastic modulus  $E_\infty$ . Notice that Eq. (9) can be rephrased as

$$\frac{1}{2} \left( \frac{\sigma_0}{E_0} \right)^2 + \kappa \frac{\sigma_0}{E_0} (1 - \cos \theta) = \kappa \frac{\Delta\gamma}{E_0 d} \quad (10)$$

where we have defined  $\kappa = E_\infty/E_0$ . For  $\theta = 0$ , we get

$$\sigma_K = \sqrt{\frac{2\kappa E_0 \Delta\gamma}{d}} = \sqrt{\frac{2E_\infty \Delta\gamma}{d}}$$

so that in this case the peeling is much more tough than in the (low frequency) elastic case and occurs as the effective work of adhesion is  $\kappa$ -times larger than  $\Delta\gamma$ .

In order to explain the appearance of the high-frequency viscoelastic modulus  $E_\infty$  in Eq. (10) we note that, because of the stuck condition assumption (no relative sliding at the tape-substrate interface), the tape is subjected to an abrupt stretching at the peeling front (see Fig. 1). This step change of the tape stress  $\sigma$  leads, regardless of the peeling velocity  $V_0$ , to a very short time (i.e. high-frequency) excitation of the viscoelastic tape.

For this reason, very close to the peeling front, the material response is governed by the high-frequency viscoelastic response, which makes the tape locally behave as a perfectly elastic material with elastic modulus  $E_\infty$ .

Notably, in real conditions, the abrupt change of the tape stress during peeling would be smoothed, as it must occur on a finite length scale across the peeling section. Since this can be estimated of order of the tape thickness  $d$  (see also Refs [54, 68]), the tape excitation frequency during peeling is approximately  $\omega \approx V_0/d$ , so that at very low peeling velocities, i.e. when  $V_0 \ll d/t_c$ , the tape response would be governed by the low-frequency viscoelastic modulus  $E_0$ . However, since we expect that usually  $V_0 \gg d/t_c$ , this would not qualitatively affect our physical picture of the peeling behavior provided so far.

### A. Frictional sliding interface

The discussion provided in the previous section is based on the assumption that the tape firmly sticks to the rigid substrate, and the tangential component of the peeling force  $P$ , remotely acting on the tape tip, is locally balanced by a point reaction force acting in the peeling section. However, it has been shown that a certain amount of relative sliding occurs in real interfaces [41, 58, 69], so that the tangential component of the peeling force  $P$  is balanced by the interfacial shear stresses arising at the interface between the tape and the rigid substrate. In this case, assuming a uniform interfacial shear stress  $\tau$ , a portion of the adhering tape of length  $a = P \cos \theta / \tau b$  is gradually stretched. Such a physical scenario is shown in Fig. 2.

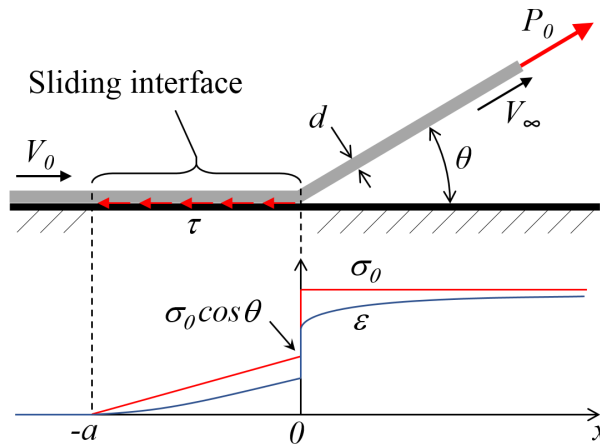


FIG. 2: The scheme of the peeling process of a thin viscoelastic layer from a rigid substrate in the presence of relative sliding at the interface. Notably,  $\tau$  is the frictional shear stress. In the lower part, qualitative diagrams of the tape stress  $\sigma$  (red) and deformation  $\varepsilon$  (blue) are shown.

The work per unit time done by interfacial frictional stresses is

$$W_T = - \int_{-a}^0 V_S(x) \tau b dx = -\tau b V_0 \int_{-a}^0 \varepsilon(x) dx \quad (11)$$

where  $V_S(x) = V_0\varepsilon(x)$  is the sliding velocity distribution at the interface. Of course the stress and deformation distributions along the tape are modified due to the presence of the tangential tractions  $\tau$ . Indeed, we have

$$\begin{aligned}\sigma(x) &= \frac{\tau}{d}(x+a); & -a \leq x < 0 \\ \sigma(x) &= \sigma_0; & x > 0\end{aligned}\quad (12)$$

where  $\sigma_0 \cos\theta = \tau a/d$ . From Eq. (12), recalling, Eq. (5), one obtains

$$\begin{aligned}\varepsilon(x) &= \frac{\tau}{E_0 d}(a+x) - \frac{\tau\lambda}{E_1 d} \left[ 1 - \exp\left(-\frac{x+a}{\lambda}\right) \right]; & -a \leq x < 0 \\ \varepsilon(x) &= \frac{\sigma_0}{E_0} - \frac{\sigma_0}{E_1} \left\{ 1 - \frac{\tau a}{\sigma_0 d} + \frac{\tau\lambda}{\sigma_0 d} \left[ 1 - \exp\left(-\frac{a}{\lambda}\right) \right] \right\} \exp(-x/\lambda); & x > 0\end{aligned}\quad (13)$$

Recalling Eq. (11) and using Eqs. (12, 13) we have

$$W_T = -bdV_0 \frac{\sigma_0^2}{2E_0} \cos^2\theta \left\{ 1 - 2\frac{\kappa-1}{\kappa} \frac{\lambda}{a} \left[ 1 - \frac{\lambda}{a} + \frac{\lambda}{a} \exp\left(-\frac{a}{\lambda}\right) \right] \right\} \quad (14)$$

Note that for  $a/\lambda \rightarrow \infty$  we get  $W_T \rightarrow -\frac{1}{2}bdV_0(\sigma_0^2/E_0) \cos^2\theta$  which involves the low frequency modulus  $E_0$ ; whereas, for  $a/\lambda \rightarrow 0$  we get  $W_T \rightarrow -\frac{1}{2}bdV_0(\sigma_0^2/E_\infty)$ , which involves the high frequency modulus  $E_\infty$ . Moreover,  $W_T(a/\lambda \rightarrow \infty) = \kappa W_T(a/\lambda \rightarrow 0)$ .

This time, the work per unit time done by tape internal stresses is

$$\begin{aligned}W_I &= -bdV_0 \int_{-\infty}^{+\infty} \sigma(x) \varepsilon'(x) dx = \\ &= -bdV_0 \frac{\sigma_0^2}{2E_0} \cos^2\theta \left\{ 1 - 2\frac{\kappa-1}{\kappa} \frac{\lambda}{a} \left[ \frac{\lambda}{a} - \left( 1 + \frac{\lambda}{a} \right) \exp\left(-\frac{a}{\lambda}\right) \right] \right\} \\ &= -bdV_0 \frac{\sigma_0^2}{2\kappa E_0} (1 - \cos^2\theta) \\ &= -bdV_0 \frac{\kappa-1}{\kappa} \frac{\sigma_0^2}{E_0} \left\{ 1 - \cos\theta \left[ 1 - \frac{\lambda}{a} + \frac{\lambda}{a} \exp\left(-\frac{a}{\lambda}\right) \right] \right\}\end{aligned}\quad (15)$$

Finally, recalling that

$$W_E + W_I + W_S + W_T = 0 \quad (16)$$

and using Eqs. (2,3,14,15) into Eq. (16), the final peeling equilibrium equation for a viscoelastic tape in the presence of frictional sliding at the interface is found as

$$\begin{aligned}\frac{\sigma_0^2}{2E_0} \left\{ (1 - \cos^2\theta) - \frac{\kappa-1}{\kappa} (1 - \cos\theta) \left( 1 + 2\cos\theta \left[ \frac{\lambda}{a} \left( 1 - \exp\left(-\frac{a}{\lambda}\right) \right) - \frac{1}{2} \right] \right) \right\} \\ + \sigma_0(1 - \cos\theta) - \frac{\Delta\gamma}{d} = 0\end{aligned}\quad (17)$$

### III. RESULTS

Let us introduce the following dimensionless parameters:  $\tilde{\sigma}_0 = \sigma_0/E_0$ ,  $\tilde{\tau} = \tau/E_0$ ,  $\Delta\tilde{\gamma} = \Delta\gamma/(E_0d)$  and  $\tilde{V}_0 = V_0t_c/d$ . Note that  $a/\lambda = \tilde{\sigma}_0 \cos\theta / (\tilde{V}_0\tilde{\tau})$ . Therefore Eq. (17) becomes

$$\frac{1}{2}\tilde{\sigma}_0^2 \left\{ (1 - \cos^2\theta) - \frac{\kappa - 1}{\kappa} (1 - \cos\theta) \left( 1 + 2\cos\theta \left[ \frac{\tilde{V}_0\tilde{\tau}}{\tilde{\sigma}_0 \cos\theta} \left( 1 - \exp\left(-\frac{\tilde{\sigma}_0 \cos\theta}{\tilde{V}_0\tilde{\tau}}\right) \right) - \frac{1}{2} \right] \right) \right\} + \tilde{\sigma}_0(1 - \cos\theta) = \Delta\tilde{\gamma} \quad (18)$$

In the limiting cases of  $\tilde{V}_0 \gg 1$  and  $\tilde{\tau} \gg 1$ , Eq. (17) gives

$$\frac{1}{2} \frac{\sigma_0^2}{E_\infty} (1 - \cos^2\theta) + \sigma_0(1 - \cos\theta) = \frac{\Delta\gamma}{d} \quad (19)$$

which clearly differs from Eq. (9), and shows that the energy dissipation due to frictional sliding at the interface is proportional to  $\frac{1}{2}(\sigma_0^2/E_\infty)\cos^2\theta$ , and leads to very much tougher peeling process at small peeling angle. Indeed, Frictional stresses causes the equilibrium stress  $\sigma_0$  to diverge as  $\sigma_K/\theta$  at small angles. This result has been already observed in Refs. [43, 70] for purely elastic tapes ( $E_0$  is replaced by  $E_\infty$ ), and can be interpreted as the emergence of an infinitely tough peeling behavior. Incidentally, it is worth noticing that ultratough peeling has been also predicted to occur when the tape is elastic and the substrate viscoelastic [33, 34].

Similarly, in the limiting case of  $\tilde{V}_0\tilde{\tau} \ll 1$  with  $\tilde{V}_0 \gg 1$  (i.e.  $V_0 \gg d/t_c$ ), Eq. (17) becomes

$$\frac{1}{2} \frac{\sigma_0^2}{E_0} (1 - \cos^2\theta) - \frac{[\sigma_0(1 - \cos\theta)]^2}{2E_1} + \sigma_0(1 - \cos\theta) = \frac{\Delta\gamma}{d}, \quad (20)$$

where the additional term

$$D_f = \frac{\sigma_0^2(1 - \cos\theta)^2}{2E_1} = (1 - \cos\theta)^2 D_s \quad (21)$$

represents the viscoelastic energy dissipation per unit time associated with the tape viscoelastic process relaxation, triggered by the stress step change  $\Delta\sigma = \sigma_0 - \sigma_0 \cos\theta$ , which occurs at the peeling front. Indeed, this time Eq. (8) is still valid provided that  $\sigma_0$  is replaced by  $\Delta\sigma$ . Notice that, as already discussed before, for  $\tilde{V}_0 \ll 1$  (i.e.  $V_0 \ll d/t_c$ ) the term  $D_f$  must also vanish, as the tape behaves elastically with modulus  $E_0$ . Therefore, for  $\tilde{\tau} \ll 1$  and  $\tilde{V}_0 \ll 1$  (i.e.  $V_0 \ll d/t_c$ ), Eq. (17) becomes

$$\frac{1}{2} \frac{\sigma_0^2}{E_0} (1 - \cos^2\theta) + \sigma_0(1 - \cos\theta) = \frac{\Delta\gamma}{d} \quad (22)$$

which holds true for purely elastic tapes (with elastic modulus  $E = E_0$ ) in the presence of interfacial frictional sliding (see Refs [43, 70]).

Figures 3 shows the dimensionless peeling stress  $\tilde{\sigma}_0$  as a function of the peeling angle  $\theta$ , for both stuck and sliding interfaces and different values of the parameter  $\kappa = E_\infty/E_0$  [Fig. 3a], and of the energy of adhesion  $\Delta\gamma$  [Fig. 3b].



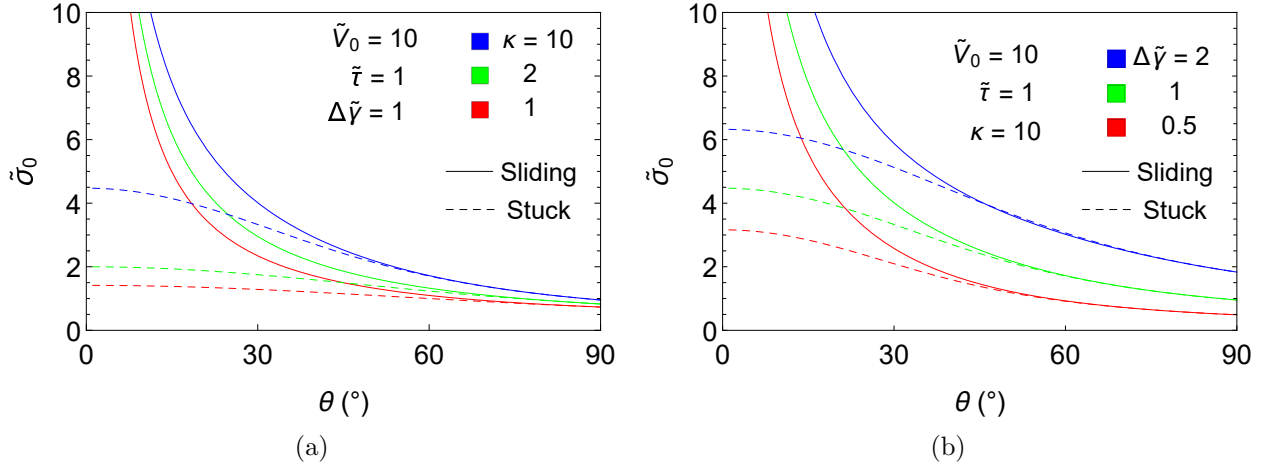


FIG. 3: The dimensionless peeling stress  $\tilde{\sigma}_0$  as a function of the peeling angle  $\theta$ , for different values of (a) the viscoelasticity parameter  $\kappa = E_\infty/E_0$ ; and (b) the dimensionless energy of adhesion  $\Delta\tilde{\gamma}$ . The dashed curves refer to the case of stuck interface between the tape and the rigid substrate, whereas continuous curves refer to frictionally sliding interfaces.

As already discussed, for the stuck case (dashed lines in Figure 3) we recover the well-known elastic Kendall's solution, where the elastic modulus is replaced by the high-frequency viscoelastic modulus  $E_\infty$  [see Eq. (10)]. Noteworthy, given the values of the low-frequency viscoelastic modulus  $E_0$ , the peeling angle  $\theta$  and work of adhesion  $\Delta\gamma$ , the peeling force increases with the parameter  $\kappa = E_\infty/E_0$ .

On the other hand, in case of frictional sliding at the interface a very different scenario emerges. This time, the peeling process is governed by Eq. (17), which, regardless the value of  $\kappa$ , leads to unbounded peeling forces for vanishing peeling angle  $\theta$  (see continuous lines in Figures 3). In this case indeed the dimensionless peeling stress obeys the equation  $\tilde{\sigma}_0 = \sqrt{2\Delta\tilde{\gamma}}/\theta$  for  $\theta \rightarrow 0$ . Interesting, such a result is in agreement with several experimental observations on the peeling behavior of insects pads in the presence of relative frictional sliding between the fibrils and the substrate [46, 59, 69]. Figure 3 presents the effect of the dimensionless energy of adhesion  $\Delta\tilde{\gamma}$  on the peeling behavior. As expected, regardless of the specific interface behavior, increasing  $\Delta\tilde{\gamma}$  leads to an overall tougher peeling behavior, as the necessary stress  $\tilde{\sigma}_0$  to sustain the peeling process increases [30].

Figure 4 shows the dimensionless peeling stress  $\tilde{\sigma}_0$  as a function of the peeling angle  $\theta$ . This time, different values of the dimensionless parameter  $\tilde{V}_0\tilde{\tau}$  are considered. In the same figure, we also report the purely elastic (with elastic modulus  $E = E_0$ ) solution in stuck conditions. We observe that, for relatively small values of the parameter  $\tilde{V}_0\tilde{\tau}$  and moderately large peeling angles  $\theta$ , the value of  $\tilde{\sigma}_0$ , observed in presence of frictional sliding, is lower than the value predicted in the case of stuck interface (see dashed red curve in Fig. 4). This is related to the different mechanisms of energy dissipation occurring in each case. Indeed, for a stuck interface, the only source of energy dissipation arises from the viscoelastic creep occurring in the detached branch of tape (i.e. for  $x > 0$ ). On the contrary, when dealing with interfaces where frictional relative motion occurs between the tape and the substrate, two additional sources of energy dissipation can be identified: (i)

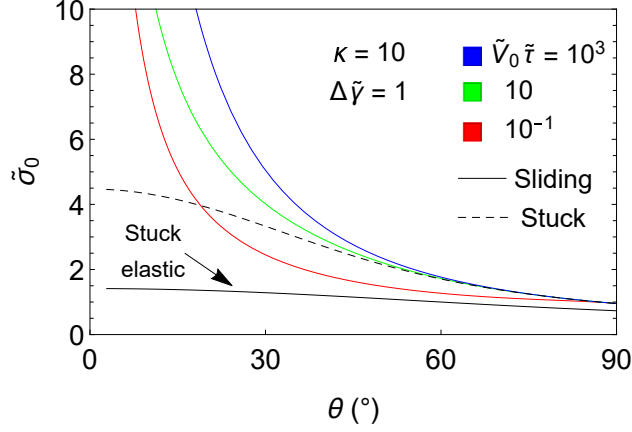


FIG. 4: The dimensionless peeling stress  $\tilde{\sigma}_0$  as a function of the peeling angle  $\theta$ , for different values of the dimensionless parameter  $\tilde{V}_0\tilde{\tau}$ . The dashed curve refers to the case of stuck interface between the tape and the rigid substrate, whereas continuum curves refer to frictionally sliding interfaces. In the same figure, we also plot for comparison the behavior of an elastic tape in stuck adhesion.

the work done by the frictional shear stress at the interface; and (ii) the viscoelastic creep occurring in the portion of the tape stretched by the interfacial frictional shear stresses (i.e. for  $-a \leq x < 0$ ). However, for  $\tilde{V}_0\tilde{\tau} < 1$  and for  $0 \ll \theta \lesssim \pi/2$ , both these terms becomes negligible as the tangential component of the peeling force is negligible as well. Under this condition, even in the case of frictionally sliding interfaces, most of the energy dissipation occurs in the detached part of the tape as a consequence of viscoelastic creep, and can be quantified as  $D_f$  through Eqs. (20, 21). Finally, since from Eq. (21) we have that  $D_f = (1 - \cos \theta)^2 D_s < D_s$ , a lower peeling force is expected for the frictional sliding case compared to stuck interfaces, as indeed shown in Fig. 4. Figure 5 shows the dimensionless

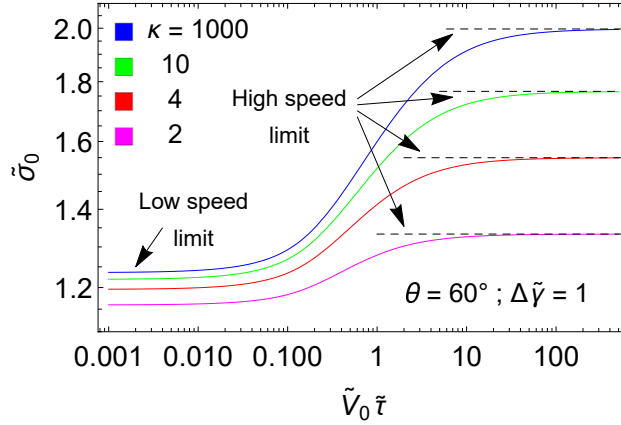


FIG. 5: The dimensionless peeling stress  $\tilde{\sigma}_0$  as a function of the dimensionless parameter  $\tilde{V}_0\tilde{\tau}$ , for different values of the parameter  $\kappa = E_\infty/E_0$ . In the figure, both the high and low speed plateau are highlighted.

peeling stress  $\tilde{\sigma}_0$  as a function of the dimensionless parameter  $\tilde{V}_0\tilde{\tau}$  for a given value of  $\theta$ . All

the cases refer to  $\tilde{V}_0 > 1$ . As expected three different regimes can be observed depending on the value of  $\tilde{V}_0\tilde{\tau}$ . For  $\tilde{V}_0\tilde{\tau} \ll 1$  an asymptotic plateau for  $\tilde{\sigma}_0$  is observed as predicted by Eq. (20), which depends on the value of  $\kappa$ . For  $\tilde{V}_0\tilde{\tau} \gg 1$ , the peeling behavior is governed by Eq. (19) and depends on the high frequency viscoelastic modulus  $E_\infty$ . Again, a plateau is observed for  $\tilde{\sigma}_0$ , whose value saturates as for  $\kappa \rightarrow \infty$  as the Rivlin's solution is approached in the case of infinitely stiff tapes. At intermediate values of  $\tilde{V}_0\tilde{\tau}$  the hysteretic viscoelastic behavior of the tape plays a key role so that, in this transition region, the peeling force increases with the peeling rate by following a power law  $\tilde{\sigma}_0 \approx (\tilde{V}_0\tilde{\tau})^n$  where the exponent  $n$  depends on the parameter  $\kappa$ .

#### IV. CONCLUSIONS

In this study, we investigate the peeling behavior of a thin viscoelastic tape peeled away from a rigid substrate. Specifically, we consider two alternative scenarios: one, with the interface between the tape and the rigid substrate in stuck adhesion (i.e. no sliding occurs); the other, assuming relative sliding on a portion of the interface in the presence of frictional shear stresses.

We found that, in stuck interfaces, the overall viscoelastic peeling behavior is independent of the peeling velocity, provided that the peeling velocity  $V_0 \gg d/t_c$  (where  $d$  is the thickness of the tape and  $t_c$  is the creep characteristic time of the viscoelastic material), and the peeling force takes the value predicted by Kendall's peeling model with the elastic modulus given by the high-frequency viscoelastic modulus  $E_\infty$  of the tape material. Under these conditions the energy dissipation associated with the viscoelastic creep of the tape is entirely localized in the detached portion of the tape.

In the presence of frictional sliding at the interface additional sources of energy dissipation come into play, which are associated with both the work done by frictional shear stress and the viscoelastic hysteresis occurring in the portion of the adhering tape subjected to forces. In such conditions, the peeling force is predicted to continuously increase as the peeling angle is decreased, leading to unbounded values for a vanishing peeling angle. Also, the viscoelastic hysteretic behavior of the tape strongly affects the dependence of the peeling force from the peeling velocity. Indeed, for any given value of the peeling angle, three regions can be identified: (i) the low velocity region, where a low plateau is reported for the peeling force; (ii) the transition region, where the peeling force increases as a power law of the peeling velocity, and (iii) the high velocity region, where a high plateau of the peeling force occurs.

**Acknowledgement 1** *This project has received funding from the European Union's Horizon 2020 research and innovation programme under the Marie Skłodowska-Curie grant agreement no. 845756 (N.M. Individual Fellowship). This work was partly supported by the Italian Ministry of Education, University and Research under the Programme "Progetti di Rilevante Interesse Nazionale (PRIN)", Grant Protocol 2017948, Title: Foam Airless Spoked Tire – FASTire (G.C.)*

- 
- [1] Hyun, S., Pei, L., Molinari, J.-F., Robbins, M.O., Finite-element analysis of contact between elastic self-affine surfaces, *Phys. Rev. E* 2004;70.
- [2] Campana C., Mueser M.H. and Robbins M.O., Elastic contact between self-affine surfaces: comparison of numerical stress and contact correlation functions with analytic predictions. *J. Phys. Condens. Matter* 2008;20(35).
- [3] Yang, C. and Persson, B.
- [4] Pastewka, L., & Robbins, M. O. Contact area of rough spheres: Large scale simulations and simple scaling laws. *Applied Physics Letters* 2016;108(22):221601.
- [5] Menga, N., L. Afferrante, and G. Carbone. Adhesive and adhesiveless contact mechanics of elastic layers on slightly wavy rigid substrates. *International Journal of Solids and Structures* 2016;88:101-109.
- [6] Müser, Martin H., et al. "Meeting the contact-mechanics challenge." *Tribology Letters* 65.4 (2017): 1-18.
- [7] Menga, N., & Carbone, G. (2019). The surface displacements of an elastic half-space subjected to uniform tangential tractions applied on a circular area. *European Journal of Mechanics-A/Solids*, 73, 137-143.
- [8] Menga, N. (2019). Rough frictional contact of elastic thin layers: The effect of geometric coupling. *International Journal of Solids and Structures*, 164, 212-220.
- [9] Persson B.N.J., Theory of rubber friction and contact mechanics, *Journal of Chemical Physics* 2001;115:3840 -3861.
- [10] Persson, B. N. J., Albohr, O., Creton, C., & Peveri, V. (2004). Contact area between a viscoelastic solid and a hard, randomly rough, substrate. *The Journal of chemical physics*, 120(18), 8779-8793.
- [11] Scaraggi, M., & Persson, B. N. J. (2015). Friction and universal contact area law for randomly rough viscoelastic contacts. *Journal of Physics: Condensed Matter*, 27(10), 105102.
- [12] Menga, N., Putignano, C., Carbone, G., & Demelio, G. P. (2014). The sliding contact of a rigid wavy surface with a viscoelastic half-space. *Proc. R. Soc. A*, 470(2169), 20140392.
- [13] Menga, N., Afferrante, L. and Carbone, G., Effect of thickness and boundary conditions on the behavior of viscoelastic layers in sliding contact with wavy profiles, *The Journal of the Mechanics and Physics of Solids* 2016;95: 517-529.
- [14] Menga, N., Afferrante, L., Demelio, G. P., & Carbone, G. (2018). Rough contact of sliding viscoelastic layers: numerical calculations and theoretical predictions. *Tribology International*, 122, 67-75.
- [15] Zhang, X., Wang, Q. J., & He, T. (2020). Transient and steady-state viscoelastic contact responses of layer-substrate systems with interfacial imperfections. *Journal of the Mechanics and Physics of Solids*, 145, 104170.
- [16] Menga, N., Carbone, G., & Dini, D. (2021). Exploring the effect of geometric coupling on friction and energy dissipation in rough contacts of elastic and viscoelastic coatings. *Journal of the Mechanics and Physics of Solids*, 148, 104273.
- [17] Carbone, G., & Mangialardi, L. (2008). Analysis of the adhesive contact of confined layers by using a Green's function approach. *Journal of the Mechanics and Physics of Solids*, 56(2), 684-706.
- [18] Martina, D., Creton, C., Damman, P., Jeusette, M., & Lindner, A. (2012). Adhesion of soft

- viscoelastic adhesives on periodic rough surfaces. *Soft Matter*, 8(19), 5350-5357.
- [19] Pastewka, L., & Robbins, M. O. (2014). Contact between rough surfaces and a criterion for macroscopic adhesion. *Proceedings of the National Academy of Sciences*, 111(9), 3298-3303.
- [20] Medina S. and Dini D., A numerical model for the deterministic analysis of adhesive rough contacts down to the nano-scale. *International Journal of Solids and Structures* 2014;51(14):2620-2632.N.J., *Molecular Dynamics Study of Contact Mechanics: Contact Area and Interfacial Separation from Small to Full Contact*, *Phys. Rev. Lett.* 2008;100.
- [21] Rey, V., Anciaux, G., & Molinari, J. F. (2017). Normal adhesive contact on rough surfaces: efficient algorithm for FFT-based BEM resolution. *Computational Mechanics*, 60(1), 69-81.
- [22] Menga, N., Carbone, G., & Dini, D. Do uniform tangential interfacial stresses enhance adhesion? *Journal of the Mechanics and Physics of Solids* 2018;112:145-156.
- [23] Menga, N., Carbone, G., & Dini, D. (2019). Corrigendum to: "Do uniform tangential interfacial stresses enhance adhesion?". *Journal of the Mechanics and Physics of Solids* 2019;133:103744. Doi: <https://doi.org/10.1016/j.jmps.2019.103744>
- [24] Menga, N., Putignano, C., Afferrante, L., & Carbone, G. (2019). The Contact Mechanics of Coated Elastic Solids: Effect of Coating Thickness and Stiffness. *Tribology Letters*, 67(1), 24.
- [25] Zhu, Z., Xia, Y., Jiang, C., Yang, Z., & Jiang, H. (2021). Investigation of zero-degree peeling behavior of visco-hyperelastic highly stretchable adhesive tape on rigid substrate. *Engineering Fracture Mechanics*, 241, 107368.
- [26] Creton, C., & Ciccotti, M. (2016). Fracture and adhesion of soft materials: a review. *Reports on Progress in Physics*, 79(4), 046601.
- [27] Kaelble, D. H. (1959). Theory and analysis of peel adhesion: mechanisms and mechanics. *Transactions of the Society of Rheology*, 3(1), 161-180.
- [28] Kaelble, D. H. (1960). Theory and analysis of peel adhesion: bond stresses and distributions. *Transactions of the Society of Rheology*, 4(1), 45-73.
- [29] Kaelble, D. H. (1965). Peel Adhesion: Micro-Fracture Mechanics of Interfacial Unbonding of Polymers. *Transactions of the Society of Rheology*, 9(2), 135-163.
- [30] Kendall, K., 1975, Thin-film peeling-the elastic term, *J. Phys. D: Appl Phys* 8, 1449-1452.
- [31] Kendall, K. (1973). Peel adhesion of solid films-the surface and bulk effects. *The Journal of Adhesion*, 5(3), 179-202.
- [32] Kendall, K. (1973). The shapes of peeling solid films. *The Journal of Adhesion*, 5(2), 105-117.
- [33] Afferrante, L., & Carbone, G. (2016). The ultratough peeling of elastic tapes from viscoelastic substrates. *Journal of the Mechanics and Physics of Solids*, 96, 223-234.
- [34] Pierro, E., Afferrante, L., & Carbone, G. (2020). On the peeling of elastic tapes from viscoelastic substrates: Designing materials for ultratough peeling. *Tribology International*, 146, 106060.
- [35] Derail, C., Allal, A., Marin, G., & Tordjeman, P. (1997). Relationship between viscoelastic and peeling properties of model adhesives. Part 1. Cohesive fracture. *The Journal of Adhesion*, 61(1-4), 123-157.
- [36] Zhou, M., Tian, Y., Pesika, N., Zeng, H., Wan, J., Meng, Y., & Wen, S. (2011). The extended peel zone model: effect of peeling velocity. *The Journal of Adhesion*, 87(11), 1045-1058.
- [37] Chen, H., Feng, X., Huang, Y., Huang, Y., & Rogers, J. A. (2013). Experiments and viscoelastic analysis of peel test with patterned strips for applications to transfer printing. *Journal of the Mechanics and Physics of Solids*, 61(8), 1737-1752.
- [38] Peng, Z., Wang, C., Chen, L., & Chen, S. (2014). Peeling behavior of a viscoelastic thin-film on a rigid substrate. *International Journal of Solids and Structures*, 51(25-26), 4596-4603.

- [39] Kendall, K. (1975). Crack propagation in lap shear joints. *Journal of Physics D: Applied Physics*, 8(5), 512.
- [40] Kendall, K. (1978). Interfacial dislocations spontaneously created by peeling. (Adhesive joint strength). *Journal of Physics D: Applied Physics*, 11(11), 1519.
- [41] Newby, B. M. Z., Chaudhury, M. K., & Brown, H. R. (1995). Macroscopic evidence of the effect of interfacial slippage on adhesion. *Science*, 269(5229), 1407-1409.
- [42] Zhang Newby, B. M., & Chaudhury, M. K. (1997). Effect of interfacial slippage on viscoelastic adhesion. *Langmuir*, 13(6), 1805-1809.
- [43] Begley, M. R., Collino, R. R., Israelachvili, J. N., & McMeeking, R. M. (2013). Peeling of a tape with large deformations and frictional sliding. *Journal of the Mechanics and Physics of Solids*, 61(5), 1265-1279.
- [44] Wang, S. J., & Li, X. (2007). The effects of tensile residual stress and sliding boundary on measuring the adhesion work of membrane by pull-off test. *Thin solid films*, 515(18), 7227-7231.
- [45] Autumn K, Hsieh S, Dudek D, Chen J, Chitaphan C, Full R.J. 2006 Dynamics of geckos running vertically. *J. Exp. Biol.* 209, 260–272. (doi:10.1242/jeb.01980)
- [46] Autumn, K., Dittmore, A., Santos, D., Spenko, M., & Cutkosky, M. (2006). Frictional adhesion: a new angle on gecko attachment. *Journal of Experimental Biology*, 209(18), 3569-3579.
- [47] Tian Y, Pesika N, Zeng H, Rosenberg K, Zhao B, McGuiggan P, Autumn K, Israelachvili J. 2006 Adhesion and friction in gecko toe attachment and detachment. *Proc. Natl Acad. Sci. USA* 103, 19 320–19 325. (doi:10.1073/pnas.0608841103)
- [48] Endlein T, Federle W. 2013 Rapid reflexes in smooth adhesive pads of insects prevent sudden detachment. *Proc. R. Soc. B* 280, 20122868. (doi:10.1098/rspb.2012.2868)
- [49] Endlein T, Ji A, Samuel D, Yao N, Wang Z, Barnes WJP, Federle W, Kappl M, Dai Z. 2013 Sticking like sticky tape: tree frogs use friction forces to enhance attachment on overhanging surfaces. *J. R. Soc. Interface* 10, 20120838. (doi:10.1098/rsif.2012.0838)
- [50] Gao, H., Wang, X., Yao, H., Gorb, S., & Arzt, E. (2005). Mechanics of hierarchical adhesion structures of geckos. *Mechanics of Materials*, 37(2-3), 275-285.
- [51] Lee, D. Y., Lee, D. H., Lee, S. G., & Cho, K. (2012). Hierarchical gecko-inspired nanohairs with a high aspect ratio induced by nanoyielding. *Soft Matter*, 8(18), 4905-4910.
- [52] Zhao, H. P., Wang, Y., Li, B. W., & Feng, X. Q. (2013). Improvement of the peeling strength of thin films by a bioinspired hierarchical interface. *International Journal of Applied Mechanics*, 5(02), 1350012.
- [53] Heepe, L., Raguseo, S., & Gorb, S. N. (2017). An experimental study of double-peeling mechanism inspired by biological adhesive systems. *Applied Physics A*, 123(2), 124.
- [54] Menga, N., Afferrante, L., Pugno, N. M., & Carbone, G. (2018). The multiple V-shaped double peeling of elastic thin films from elastic soft substrates. *Journal of the Mechanics and Physics of Solids*, 113, 56-64.
- [55] Menga, N., Dini, D., & Carbone, G. (2020). Tuning the periodic V-peeling behavior of elastic tapes applied to thin compliant substrates. *International Journal of Mechanical Sciences*, 170, 105331.
- [56] Afferrante, L., Carbone, G., Demelio, G., & Pugno, N. (2013). Adhesion of elastic thin films: double peeling of tapes versus axisymmetric peeling of membranes. *Tribology Letters*, 52(3), 439-447.
- [57] Labonte D, Federle W. 2013 Functionally different pads on the same foot allow control of attachment: stick insects have load-sensitive ‘heel’ pads for friction and shear-sensitive ‘toe’

- pads for adhesion. PLoS ONE 8, e81943. (doi:10.1371/journal.pone.0081943)
- [58] Amouroux N, Petit J, Le´ger L. 2001 Role of interfacial resistance to shear stress on adhesive peel strength. *Langmuir* 17, 6510–6517. (doi:10.1021/la010146r)
- [59] Labonte, D., & Federle, W. (2016). Biomechanics of shear-sensitive adhesion in climbing animals: peeling, pre-tension and sliding-induced changes in interface strength. *Journal of The Royal Society Interface*, 13(122), 20160373.
- [60] Chen B, Wu P, Gao H. 2009 Pre-tension generates strongly reversible adhesion of a spatula pad on substrate. *J. R. Soc. Interface* 6, 529–537. (doi:10.1098/rsif.2008.0322)
- [61] Williams J. 1993 A review of the determination of energy release rates for strips in tension and bending. Part I—static solutions. *J. Strain Anal. Eng.* 28, 237–246. (doi:10.1243/03093247V284237)
- [62] Labonte D, Federle W. 2015 Rate-dependence of ‘wet’ biological adhesives and the function of the pad secretion in insects. *Soft Matter* 11, 8661–8673. (doi:10.1039/C5SM01496D)
- [63] Federle, W., Riehle, M., Curtis, A. S., & Full, R. J. (2002). An integrative study of insect adhesion: mechanics and wet adhesion of pretarsal pads in ants. *Integrative and Comparative Biology*, 42(6), 1100-1106.
- [64] Federle, W., Baumgartner, W., & Hölldobler, B. (2004). Biomechanics of ant adhesive pads: frictional forces are rate- and temperature-dependent. *Journal of Experimental Biology*, 207(1), 67-74.
- [65] Gorb, S., Jiao, Y., & Scherge, M. (2000). Ultrastructural architecture and mechanical properties of attachment pads in *Tettigonia viridissima* (Orthoptera Tettigoniidae). *Journal of Comparative Physiology A*, 186(9), 821-831.
- [66] Puthoff, J. B., Holbrook, M., Wilkinson, M. J., Jin, K., Pesika, N. S., & Autumn, K. (2013). Dynamic friction in natural and synthetic gecko setal arrays. *Soft Matter*, 9(19), 4855-4863.
- [67] Christensen R. M., *Theory of viscoelasticity*, Academic Press, New York, 1982.
- [68] Lin, Y., & Freund, L. B. (2007). Forced detachment of a vesicle in adhesive contact with a substrate. *International journal of solids and structures*, 44(6), 1927-1938.
- [69] Collino, R. R., Philips, N. R., Rossol, M. N., McMeeking, R. M., & Begley, M. R. (2014). Detachment of compliant films adhered to stiff substrates via van der Waals interactions: role of frictional sliding during peeling. *Journal of The Royal Society Interface*, 11(97), 20140453.
- [70] Jagota, A., & Hui, C. Y. (2011). Adhesion, friction, and compliance of bio-mimetic and bio-inspired structured interfaces. *Materials Science and Engineering: R: Reports*, 72(12), 253-292.